Identification of contaminant sources in enclosed environments by inverse CFD modeling

T. F. Zhang, Q. Chen[*]

Air Transportation Center of Excellence for Airliner Cabin Environmental Research (ACER),
School of Mechanical Engineering, Purdue University,
585 Purdue Mall, West Lafayette, IN 47907-2088, USA

Abstract

In case contaminants are found in enclosed environments such as aircraft cabins or buildings, it is useful to find the contaminant sources. One method to locate contaminant sources is by inverse computational fluid dynamics (CFD) modeling. Since the inverse CFD modeling is ill-posed, this paper has proposed to solve a quasi-reversibility (QR) equation for contaminant transport. The equation improves the numerical stability by replacing the second-order diffusion term with a fourth-order stabilization term in the governing equation of contaminant transport. In addition, a numerical scheme for solving the QR equation in unstructured meshes has been developed. This paper demonstrates how to use the inverse CFD model with the QR equation and numerical scheme to identify gaseous contaminant sources in a two-dimensional aircraft cabin and in a three-dimensional office. The inverse CFD model could identify the contaminant source locations but not very accurate contaminant source strength due to the dispersive property of the QR equation. The results also show that this method works better for convection dominant flows than the flows that convection is not so important.

Keywords: Inverse modeling; Quasi-reversibility equation; CFD; Numerical stability; Enclosed environment.

Practical Implications

The paper presents a methodology that can be used to find contaminant source locations and strengths in enclosed environments with the data of airflow and contaminants measured by sensors. The method can be a very useful tool to find where, what, and how contamination has happened. The results can be used to develop appropriate measures to protect occupants in the enclosed environments from infectious diseases or terrorist releases of chemical/biological warfare agents as well as to decontaminate the environments.

Nomenclature

---

[*] Corresponding author tel.: (765) 496-7562; Fax: (765) 496-7534; email: yanchen@purdue.edu

$\vec{A}$	Area vector	Δx	Grid size in one-dimensional airflow
ds	Distance between two neighboring cell centers	$\Delta \tau$	Negative time step
ds_i	Projection of ds along direction i	Γ	Diffusion coefficient of gaseous contaminant scalar
$\hat{e}_s$	Unit vector connecting two neighboring cell centers	ε	Stabilization constant
$\hat{e}_t$	Unit vector along the tangent face direction	ϕ	Gaseous contaminant scalar
J	Mass flow rate	ρ	Air density
u_i	Velocity component in direction i	τ	Time
u	Velocity in one-dimensional airflow		
x_i	Coordinate in direction i		
		Subscripts	
		i	Coordinate direction index
Greek symbols		f	Face index in an unstructured grid
ΔV	Control volume		

Introduction

In case contaminants are found in enclosed environments such as aircraft cabins or buildings, it is useful to find the contaminant sources so that appropriate actions can be taken. For example, if we could identify the index person who spread the Sever Acute Respiratory Syndrome (SARS) virus in the flight from Hong Kong to Beijing in 2003 (Olsen et al., 2003), emergent measures could be taken to protect other passengers from the infection. It would be also supercritical for us to know the source location in a building in case of chemical/biological warfare agent release from a terrorist attack. Sensors can measure the distributions of airflow and contaminant concentrations in an enclosed environment. By using the distributions of contaminant concentrations as initial conditions and other boundary conditions, one can solve reversely contaminant transport so it is possible to find the source location and strength.

Computational Fluid Dynamics (CFD) has been a useful tool for the computations of airflow and contaminant transport in enclosed environments. To solve the distributions of contaminant concentrations needs boundary conditions, initial conditions, thermo-physical properties and geometric characteristics of the enclosed environments. In this cause-effect relationship of contaminant transport, the cause is boundary conditions, initial conditions, thermo-physical properties and geometric characteristics of the enclosed environment and the effect is contaminant concentration distributions. Traditionally, CFD is used to explore the cause-effect relationship that is called direct modeling. Inverse modeling is to find the causal characteristics such as the contaminant source location and strength from the finite effectual information like the distributions of airflow and contaminant concentrations.

According to different causal characteristics, the inverse modeling can be categorized into boundary, retrospective, coefficient, and geometric problems (Alifanov, 1994). Boundary problems are to find the boundary conditions that form a certain contaminant concentration

field; retrospective problems (time reversed problems) are to find the initial conditions; coefficient problems are to find some coefficients in the governing equation, for example the diffusion coefficient of contaminant transport; and geometric problems are to reconstruct the geometric characteristics of a domain. The cases of identifying the contaminant source location and strength mentioned previously are the retrospective problems. The identification of a contaminant source includes the determination of the contaminant source location and strength.

Direct CFD modeling (forward-time simulation) is well-posed, since it satisfies solution existence, uniqueness, and stability (Tikhonov and Arsenin, 1977). Unlike direct modeling, inverse CFD modeling cannot be reproduced in experiments so the relationship of cause-effect cannot be physically reversed. For inverse modeling of contaminant transport in enclosed environments, the solution physically exists since everything happens with a reason. However, the solution may not be unique because different causes may lead to the same effect. A common method to make the solution unique is by making assumptions of some unknown casual characteristics (Atmadja and Bagtzoglou, 2001). Alifanov (1994) pointed out that inverse modeling has stability problems. Since inverse CFD modeling cannot satisfy solution stability, it is ill-posed.

Although very little inverse modeling has been conducted for enclosed environments, many studies have handled ill-posed inverse modeling in heat transfer (Alifanov, 1994), groundwater transport (Sun, 1994), and atmospheric constituent transport (Enting, 2002). Inverse modeling can be categorized into analytical, optimization, probabilistic, and direct approach.

The analytical approach requires analytical solution of the distributions of airflow and contaminant concentrations. The causal characteristics are then inversely solved. The analytical approach has been successfully applied to multi-dimensional heat conduction problems (Alifanov, 1994). In groundwater transport, the analytical approach has been used to solve contaminant transport in one-dimensional flow (Alapati and Kabala, 2000) or in two-dimensional uniform flow (Ala and Domenico, 1992). The analytical approach has also been used to solve an inverse atmospheric transport problem in three-dimensional uniform flow (Kathirgamanathan et al., 2002). The analytical approach can be accurate and efficient. However, the analytical approach is only for simple problems so that the applications of the analytical approach are very limited.

The optimization approach uses direct modeling to obtain the effectual data such as distributions of contaminant concentrations based on all possible causal characteristics. Then the approach optimizes a solution that is best-fitted with the corresponding measured data. This approach has been widely applied in identifying groundwater pollution source as linear optimization method (Gorelick et al., 1983), maximum likelihood method (Wagner, 1992), and nonlinear optimization method (Mahar and Datta, 2000). Because plausible combinations of possible causal characteristics are huge, this approach involves a large amount of direct modeling.

The probabilistic approach also does direct modeling. The approach uses probability to express a possible causal aspect. Similar to the optimization approach, all possible causal characteristics should be known before doing the direct modeling. In groundwater transport, Bagtzoglou et al. (1992) and Wilson and Liu (1994) calculated the possibility of a contaminant source in groundwater by reversing only the convective contaminant transport. Snodgrass and Kitanidis (1997) used Bayesian theory to interpret the possibility of each

contaminant source. In enclosed environment, Sohn et al. (2002) also used Bayesian probability model to identify the contaminant source in a five-room building. They used a multi-zonal model to calculate the airflow and contaminant transport. Arvelo et al. (2002) used a modified multi-zone model to study the optimal placement of chemical/biological warfare agent sensors in a building with nine offices and a hallway. The optimal sensor locations should be in the spaces where most possible sources of chemical/biological warfare agent could be located so the sensors can detect the agent in the least amount of time. Different from the previous researchers, they used the genetic algorithm to interpret the computed data to locate the sources. Since the multi-zone model can only provide some macroscopic information about the contaminant transport, it is necessary to run CFD simulations if more accurate and detailed information is needed. In addition, both the probability and optimization approaches need a huge amount of direct modeling.

The direct approach solves inverse problems by reversing directly the governing equations that describe cause-effect relations. Since the reversed governing equations are unstable, the regularization technique (Tikhonov and Arsenin, 1977) or the stabilization technique (Lattes and Lions, 1969) has been used to improve the solution stability. The regularization technique improves the solution stability by imposing a bound on the solution. The solution is obtained by minimizing the objective function with a regularized term. The stabilization technique introduces some stabilization terms into the reversed governing equations or solves some auxiliary equations to improve the solution stability. In atmospheric contaminant transport modeling without using the regularization or stabilization technique, Kato et al. (2001; 2002; 2004) assessed local pollution from upwind regions by backward trajectory analysis of the flows. The method reversed only the contaminant transport by convection. This method is very easy to be implemented and can be used to roughly evaluate contaminant sources. However, neglecting the diffusion can be a problem when the convection is weak. The direct approach needs far less information about contaminant sources than the optimization and probabilistic approaches and can solve far more complicated problems than the analytical approach. Thus, the direct approach will be used in the present study.

The quasi-reversibility (QR) method belongs to the direct approach using stabilization technique. The method avoids solving the irreversible governing equation and instead solves a similar equation with a stable solution scheme. The QR method was first presented to solve ill-posed partial differential equations for heat conduction problems (Lattes and Lions, 1969). It was also used to solve the inverse heat conduction in a quasi-boundary-value-problem variant of the original formulation (Clark and Oppenheimer, 1994). Later this method was applied to solve contaminant transport in groundwater. Skaggs and Kabala (1995) used the QR method to identify groundwater contaminant sources. They concluded that the method used less computational effort than the regularization technique. Bagtzoglou and Atmadja (2003) also studied the QR method to determine contaminant sources. Their results show that the method performs well even if the initial data was with uncertainty.

The principle of contaminant transport in groundwater is similar to that in enclosed environments. The above literature review suggests that inverse modeling with the QR method is very promising for identifying contaminant sources in enclosed environments. This study has thus used the QR method to identify contaminant source location and strength in a two-dimensional aircraft cabin and in a three-dimensional office.

Theory of Inverse Modeling

This section presents the fundamentals of a new QR equation and numerical scheme for identifying contaminant source and strength in enclosed environments based on distributions of airflow and initial contaminant concentrations.

The quasi-reversibility equation

Contaminants transported in enclosed environments can be in gas, liquid, and solid phase. This paper concerns only gaseous contaminant transport for simplicity. The governing transport equation for a gaseous contaminant without a source within a period of $[0, T]$ is,

$$\frac{\partial[\phi(\tau)]}{\partial \tau} = -\frac{\partial}{\partial x_i}[u_i \phi(\tau)] + \frac{\partial}{\partial x_i}\left[\frac{\Gamma}{\rho}\frac{\partial \phi(\tau)}{\partial x_i}\right] \tag{1}$$

The left hand side of the above equation is the contaminant concentration change rate, and the right hand side of the equation is the convection and diffusion terms, respectively. If the contaminant transport equation is solved inversely, the solution is numerically unstable.

Let us analyze the contaminant transport in one-dimensional airflow shown as in Figure 1. There are five nodes *WW*, *W*, *P*, *E* and *EE* in the domain. For simplicity, the diffusion coefficient is assumed to be constant. By using the first-order upwind scheme and implicit format, Equation 1 can be discretized into,
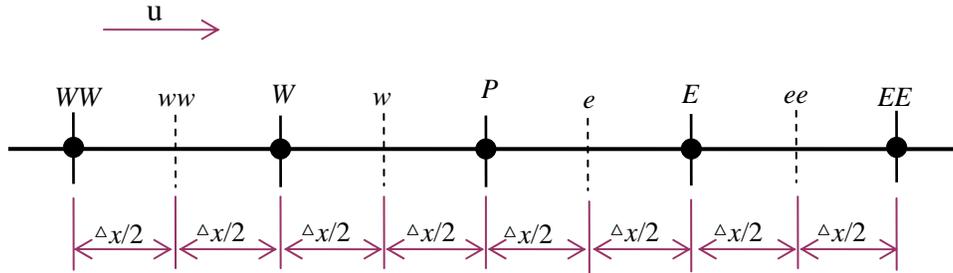
Fig. 1 The control volumes used to illustrate contaminant transport in a one-dimensional airflow

$$\phi_P(\tau+\Delta\tau) = \frac{\dfrac{u_w \Delta\tau}{\Delta x} + \dfrac{\Gamma\Delta\tau}{\rho(\Delta x)^2}}{1 + \dfrac{u_e \Delta\tau}{\Delta x} + \dfrac{2\Gamma\Delta\tau}{\rho(\Delta x)^2}}\phi_W(\tau+\Delta\tau) + \frac{\dfrac{\Gamma\Delta\tau}{\rho(\Delta x)^2}}{1 + \dfrac{u_e \Delta\tau}{\Delta x} + \dfrac{2\Gamma\Delta\tau}{\rho(\Delta x)^2}}\phi_E(\tau+\Delta\tau) +$$

$$\frac{1}{1 + \dfrac{u_e \Delta\tau}{\Delta x} + \dfrac{2\Gamma\Delta\tau}{\rho(\Delta x)^2}}\phi_P(\tau) \tag{2}$$

To calculate contaminant transport at the previous time in inverse modeling, the time step, $\Delta\tau$, in Equation 2 should be negative. The negative time step makes the coefficient of $\phi_P(\tau)$ greater than one so the calculation errors would be amplified as time elapsed in negative direction. Thus, Equation 2 is unstable in inverse modeling. In addition, the contaminant concentration at cell P shown as the left hand side of Equation 2 is unbounded by those in its neighboring cells W and E since the coefficients for $\phi_W(\tau+\Delta\tau)$ and $\phi_E(\tau+\Delta\tau)$ are negative.

In order to make the governing equation solvable with numerical stability, this study proposes a QR equation that is slightly different from the previous ones (Skaggs and Kabala, 1995; Bagtzoglou and Atmadja, 2003),

$$\frac{\partial[\phi(\tau)]}{\partial\tau} = -\frac{\partial}{\partial x_i}\left[u_i\phi(\tau)\right] + \varepsilon\frac{\partial^2}{\partial x_i^2}\left[\frac{\partial^2\phi(\tau)}{\partial x_i^2}\right] \tag{3}$$

In Equation 3, the diffusion term in the transport equation has been changed into a fourth-order stabilization term with a stabilization coefficient, ε. For the one-dimensional case as shown in Figure 1, the fourth-order term can be discretized into the following by using Taylor series,

$$\frac{\partial^4\phi_P}{\partial x^4} = \frac{\phi_{WW} - 4\phi_W + 6\phi_P - 4\phi_E + \phi_{EE}}{\Delta x^4} + O(\Delta x^2) \tag{4}$$

The fourth-order derivative at node P can be calculated with the values at the five neighboring nodes and this discretization has second-order accuracy. Substituting Equation 4 and discretizing the other two terms, the discretized format of Equation 3 becomes,

$$\phi_P(\tau+\Delta\tau) = \frac{\dfrac{\varepsilon\Delta\tau}{\Delta x^4}}{1 - \dfrac{6\varepsilon\Delta\tau}{\Delta x^4} + \dfrac{u_e\Delta\tau}{\Delta x}}\phi_{WW}(\tau+\Delta\tau) +$$

$$\frac{-\dfrac{4\varepsilon\Delta\tau}{\Delta x^4} + \dfrac{u_w\Delta\tau}{\Delta x}}{1 - \dfrac{6\varepsilon\Delta\tau}{\Delta x^4} + \dfrac{u_e\Delta\tau}{\Delta x}}\phi_W(\tau+\Delta\tau) + \frac{-\dfrac{4\varepsilon\Delta\tau}{\Delta x^4}}{1 - \dfrac{6\varepsilon\Delta\tau}{\Delta x^4} + \dfrac{u_e\Delta\tau}{\Delta x}}\phi_E(\tau+\Delta\tau) + \tag{5}$$

$$\frac{\dfrac{\varepsilon\Delta\tau}{\Delta x^4}}{1 - \dfrac{6\varepsilon\Delta\tau}{\Delta x^4} + \dfrac{u_e\Delta\tau}{\Delta x}}\phi_{EE}(\tau+\Delta\tau) + \frac{1}{1 - \dfrac{6\varepsilon\Delta\tau}{\Delta x^4} + \dfrac{u_e\Delta\tau}{\Delta x}}\phi_P(\tau)$$

The coefficient of $\phi_P(\tau)$ in Equation 5 can be smaller than one if ε is larger than $u_e\Delta x^3/6$. Then the calculation error will be lessened with time elapsed in negative direction in inverse modeling. Thus, the numerical scheme becomes stable and the equation becomes dispersive. The coefficients of $\phi_W(\tau+\Delta\tau)$ and $\phi_E(\tau+\Delta\tau)$ can also become positive so $\phi_P(\tau+\Delta\tau)$ is

bounded. Compared with Equation 2, Equation 5 has two additional terms, $\phi_{WW}(\tau + \Delta\tau)$ and $\phi_{EE}(\tau + \Delta\tau)$. The coefficients of these two terms will be negative if the denominators are positive. The negative coefficients make the contaminant concentrations at nodes *WW* and *EE* unbounded with that at node *P*. Thus, the concentration at node *P* may generate wiggles during a computation and the numerical stability may deteriorate. Nevertheless, Equation 5 may still be stable for identifying contaminant source in enclosed environments but the solution of contaminant source strength is not accurate. This is because Equation 5 is not exactly the same as the governing equation for contaminant transport. However, the total contaminant amount in the domain can be easily calculated by integrating the contaminant distributions from the initial fields and the boundary conditions.

Numerical methods

Equation 5 is only for the contaminant transport in one-dimensional airflow with uniform grid distribution. To apply the QR method in a more complicate enclosed environment, it is necessary to develop a suitable numerical scheme. Normally, a numerical scheme for unstructured meshes should work for structured meshes since structured meshes are special cases of unstructured meshes. This section presents a new numerical scheme for unstructured meshes that are more generic. The numerical scheme for solving Equation 1 in unstructured meshes was well developed in direct modeling (Mathur and Murthy, 1997). Our focus is on solving the QR equation.

Let us start from discretizing the stabilization term in the QR equation by using a generic two-dimensional domain that is presented by two triangular unstructured cells as shown in Figure 2. Cell *c*0 and *c*1 share a common face *f*. The contaminant concentration values are stored in the cell centers. ϕ_0 is the concentration for Cell *c*0, and ϕ_1 is the concentration for Cell *c*1. Mathur and Murthy (1997) determined the dot product of the concentration gradient and the face area vector to be,
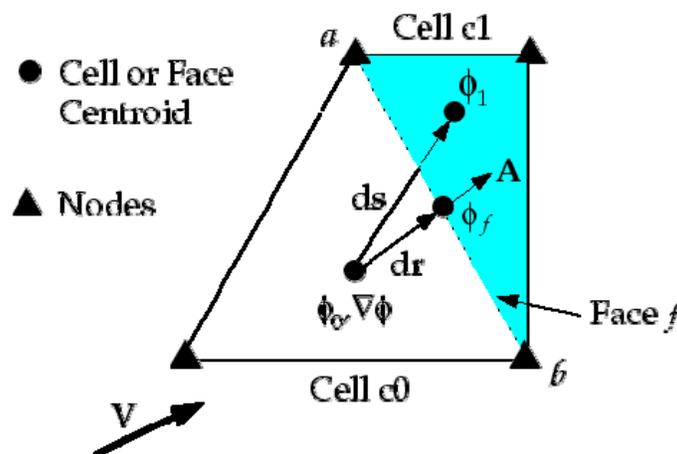
Fig. 2 Two adjacent cells c0 and c1 (Fluent Inc, 2005) in a two-dimensional flow domain

$$\vec{\nabla}\phi \cdot \vec{A} = \frac{\phi_1 - \phi_0}{ds}\frac{\vec{A}\cdot\vec{A}}{\vec{A}\cdot\hat{e}_s} + \frac{\phi_b - \phi_a}{A}\frac{\vec{A}\cdot\vec{A}}{\vec{A}\cdot\hat{e}_s}\hat{e}_t \cdot \hat{e}_s \tag{6}$$

The first term in the right hand side of Equation 6 is for the direction connecting cell centroids between the two cells. The second term of the right hand side of the equation is for the tangent face direction aligned with nodes a and b. Using Gauss's divergence theorem, the Laplacian of ϕ at cell $c0$ is,

$$\vec{\nabla}^2\phi = \frac{1}{\Delta V}\sum_f \frac{\phi_1 - \phi_0}{ds}\frac{\vec{A}\cdot\vec{A}}{\vec{A}\cdot\hat{e}_s} + \frac{1}{\Delta V}\sum_f \frac{\phi_b - \phi_a}{A}\frac{\vec{A}\cdot\vec{A}}{\vec{A}\cdot\hat{e}_s}\hat{e}_t \cdot \hat{e}_s \tag{7}$$

In the above equation, the sum of the right hand side is for all the faces of cell $c0$. The second-order derivative of concentration for cell $c0$ can be approximated as,

$$\frac{\partial^2 \phi}{\partial x_i^2} = \frac{1}{\Delta V}\sum_f \frac{ds_i}{ds}\frac{(\phi_1 - \phi_0)}{ds}\frac{\vec{A}\cdot\vec{A}}{\vec{A}\cdot\hat{e}_s} \tag{8}$$

Note in Equation 8 that the part of the second-order derivative coming from the tangent face direction has been omitted for simplicity. This approximation is acceptable for grids close to the structured grids, but may generate large errors for the unstructured grids with sharp angles. For the one-dimensional case as shown in Figure 1, Equation 8 becomes,

$$\frac{\partial^2 \phi_P}{\partial x^2} = \frac{\phi_W - 2\phi_P + \phi_E}{\Delta x^2} + O(\Delta x^2) \tag{9}$$

Equation 9 has second order accuracy. Equation 4 can be obtained by taking again the second-order derivative to Equation 9. The advantage of this discretization scheme shown in Equation 8 is that it can be easily extended to three-dimensional domains.

With the discretized expression of the stabilization term, it is necessary to discretize the other two terms in Equation 3. By integrating Equation 3 over the cell volume and time and by using backward-time implicit concentration to represent the right hand side of Equation 3, the contaminant concentration at the previous time step can be discretized as,

$$\phi(\tau + \Delta\tau) = \phi(\tau) + \frac{1}{\rho\Delta V}\left[\sum_f J_f \phi_f(\tau + \Delta\tau)\right]\Delta\tau + \varepsilon\Delta\tau\frac{\partial^2}{\partial x_i^2}\left[\frac{\partial^2\phi(\tau + \Delta\tau)}{\partial x_i^2}\right] \tag{10}$$

Note the time step, $\Delta\tau$, in the above equation is negative in inverse modeling. The second term of the right hand side of Equation 10 is the convection term. The face concentration, ϕ_f, is calculated by the linear reconstruction method (Mathur and Murthy, 1997) as,

$$\phi_f = \phi_0 + \vec{\nabla}\phi_r \cdot d\vec{r} \tag{11}$$

where $\vec{\nabla}\phi_r$ in Equation 11 is the reconstructing gradient. The gradient can be calculated with Gauss divergence theorem as,

$$\vec{\nabla}\phi_r = \frac{\alpha}{\Delta V}\sum_f \frac{\phi_0 + \phi_1}{2}\vec{A} \tag{12}$$

where α is a factor to ensure that the reconstruction does not introduce local extrema. This study has used the method proposed by Venkatakrishnan (1993) to calculate α.

In solving Equation 10, it is important to select an appropriate stabilization constant ε. Our experience shows that the ε is usually less than $ds^4/(-12\Delta\tau)$ for contaminant transport in two-dimensional enclosed environments and less than $ds^4/(-18\Delta\tau)$ for three-dimensional environments. However, to ensure the numerical stability, the ε cannot be too small.

Figure 3 shows the flow chart of the inverse modeling used in this study. Our study has embedded the QR equation and numerical scheme into a commercial CFD program, FLUENT (http://www.fluent.com/), as a user defined function according to the flow chart. The inverse modeling should always start with the known airflow and concentration distributions. The information should come from data measured by airflow and contaminant concentration sensors. For demonstration purpose, this paper used the distributions of airflow and contaminant concentration obtained from direct CFD modeling as initial data. The airflow was assumed to be steady for simplicity.

```
                          ┌──────────┐
                          │  Start   │
                          └──────────┘
```

Start

Initiate the distributions of airflow, contaminant concentration $\phi(T)$, and guess $\phi_{new}(T+\Delta\tau)$

Set $\phi_{old}(\tau+\Delta\tau) := \phi_{new}(\tau+\Delta\tau)$

Calculate the reconstructed gradient $\vec{\nabla}\phi_r$

Calculate the contaminant transported by convection

Calculate the stabilization term

Convergence
$\left|\phi_{new}(\tau+\Delta\tau) - \phi_{old}(\tau+\Delta\tau)\right| < \delta$?

No

Yes

Next time step?

Yes

No

End
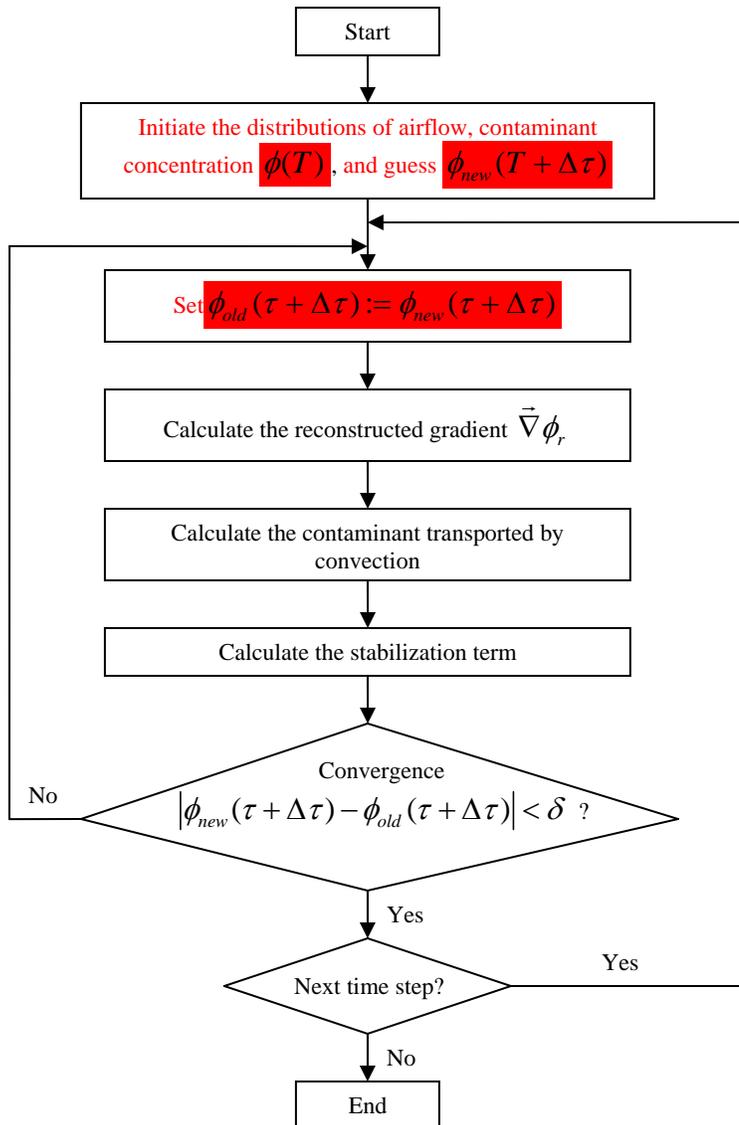
Fig. 3 Flow chart of the quasi-reversibility method

Results and discussion

The numerical methods proposed in the previous section have been used to identify contaminant sources in two cases. One is in a two-dimensional aircraft cabin, in which the unstructured meshes were used. The velocity in the cabin was very high and the contaminant transport was convection dominant. Another one is in a three-dimensional office, in which the structured meshes were used. The velocity in this office was low since it used a displacement ventilation system. The diffusion played a more important role for contaminant transport than that in the two-dimensional aircraft cabin.

Application to a two-dimensional aircraft cabin

The QR method and numerical scheme was tested in a two-dimensional empty aircraft cabin as shown in Figure 4. The airflow in an aircraft cabin is close to two dimensional. Many contaminant sources in the cabin, such as ozone and pesticide, could also be closed to two dimensional. Three-dimensional contaminants, such as viruses from a coughing passenger, are very complicated so they should be considered in another paper. The aircraft cabin was 4.72 m in width and 2.10 m in height. Conditioned air was supplied from the two slot inlets at the ceiling, and the air was extracted from the two outlets at the side walls near the floor level. There was no heat generation in this cabin so the airflow in the cabin can be considered as isothermal. A contaminant source was released at the cabin floor from $t = 0 - 0.04$ s. The geometry and flow domain of the aircraft cabin was created with unstructured meshes with *Pave* scheme. The grid size was around 0.05 m.
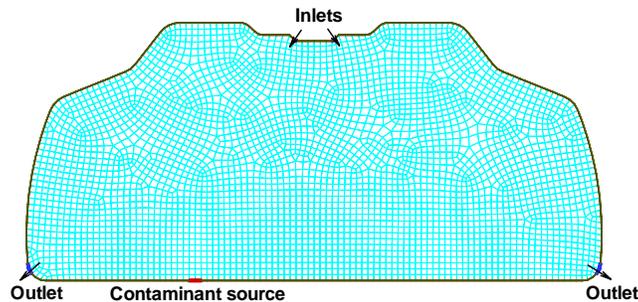
Fig. 4 Geometry and grid distribution of a two-dimensional aircraft cabin

As discussed in the previous section, the inverse modeling needs initial distributions of airflow and contaminant concentration, boundary conditions, thermo-physical properties and geometric characteristics of the enclosed environment. The boundary conditions, thermo-physical properties and geometric characteristics were known for the cabin. This study used FLUENT to obtain the distributions of airflow and contaminant concentration as initial data. The authors have realized that in practical inverse modeling the initial data can only be obtained by sensors. Since this paper is to demonstrate the performance of the QR method and numerical scheme, it is appropriate to use direct CFD modeling here to generate initial data.

FLUENT solved a set of governing partial differential RANS (Reynolds-averaged Navier-Stokes) equations with boundary conditions, thermo-physical properties and geometric characteristics of the two-dimensional cabin. These governing equations include continuity, momentum, contaminant concentration, turbulent kinetic energy, and dissipation rate of turbulent kinetic energy. The renormalization group (RNG) k-ε model was used for the turbulent flow. These partial differential equations were discretized into algebraic equations by using the finite volume method with a second-order upwind scheme. Because the equations are highly nonlinear, iterations were needed to achieve a converged airflow solution. According to the guideline for using CFD to indoor environment modeling (Chen and Srebric, 2002), the CFD results should be validated. The validation has been reported in our other paper (Zhang and Chen, 2005) with a good accuracy. By using the direct CFD modeling, Figure 5 shows the computed airflow pattern under steady state. The air from both ceiling

inlets curved toward the cabin walls on both sides of the cabin. The air jet then flowed along the floor and mixed in the middle of the cabin. Two vortexes were created in the cabin.

With the steady-state airflow pattern, direct CFD modeling was used to calculate contaminant concentration distribution at $t = 6$ s where a contaminant source was released at the floor from $t = 0 – 0.04$ s. The distributions of steady-state airflow and transient contaminant concentration at $t = 6$ s were used as initial data for the inverse CFD modeling. The inverse CFD modeling calculated backwards contaminant transport from $t = 6$ s to -2 s as shown in Figure 6(a). The computation to negative time allows us to develop a criterion about when to stop the inverse computation. In practice, $t = 0$ is normally unknown.
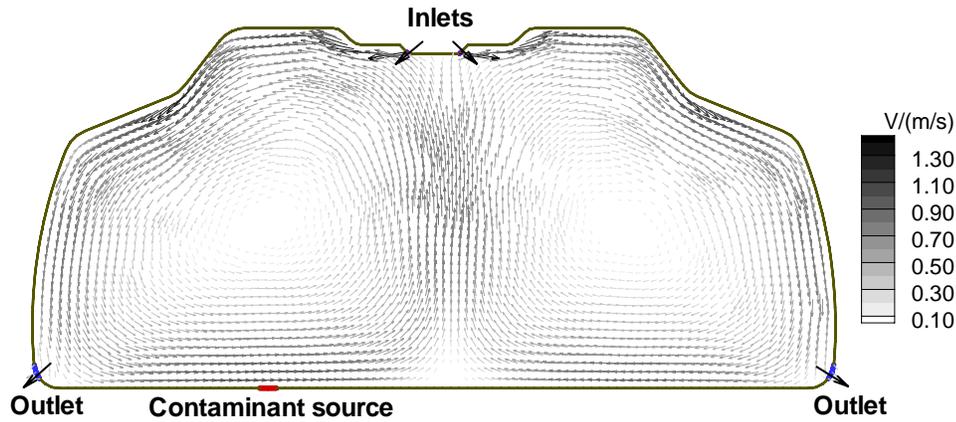
Fig. 5 The steady state airflow pattern in the two-dimensional aircraft cabin

Figure 6(b) shows the contaminant concentration distribution at $t = 6$ s computed by the direct CFD modeling (forward-time simulation). After 6 s from the release, the contaminant was mostly transported to the upper left part of the cabin. At this time no contaminant has yet been transported to the outlets.

The inverse CFD modeling used a time step of -0.04 s. The reason to use such a small time step is to ensure that the distance of the contaminant transported in one time step is less than the grid distance. The stabilization constant used was $\varepsilon=5.95\times10^{-6}$ m^4/s. Figure 7(a) shows the distribution of the contaminant concentration at $t = 0.04$ s obtained by the inverse CFD modeling. At this moment, most of the contaminant was in a narrow region on the left cabin floor. The ideal distribution should be in a small region around the contaminant source as shown in Figure 7(b). By using the maximum contaminant concentration over all locations at a given time (the peak contaminant concentration), one could identify the contaminant source. The peak contaminant concentration computed by the inverse CFD modeling in Figure 7(c) clearly shows the position of the contaminant source. Compared with the peak contaminant concentration obtained with the direct CFD modeling as shown in Figure 7(d), the source strength identified by the inverse CFD modeling is more dispersive. The reason is that the QR equation is not exactly the same as the governing transport equation for the contaminant concentration.

12
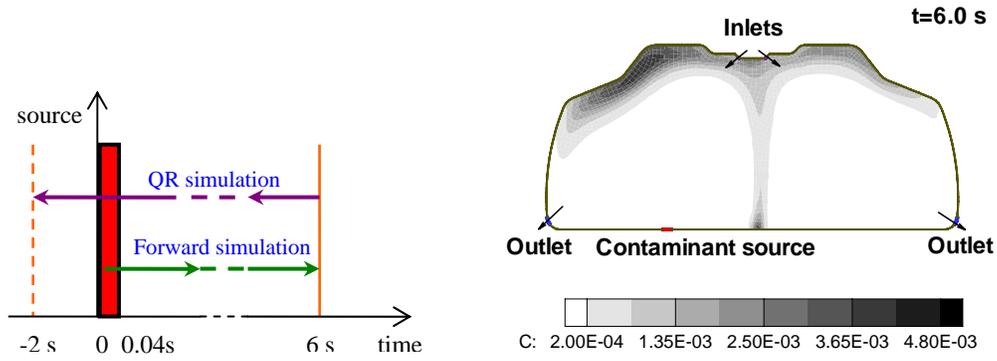
Fig. 6 Simulation schematics and the initial concentration field for backward simulation (a) Simulation schematics $t = 0$ to 6 s is for the direct CFD modeling and $t = 6$ s to -2 s is for the inverse CFD modeling, (b) the contaminant concentration distribution at t=6.0 s from the direct CFD modeling
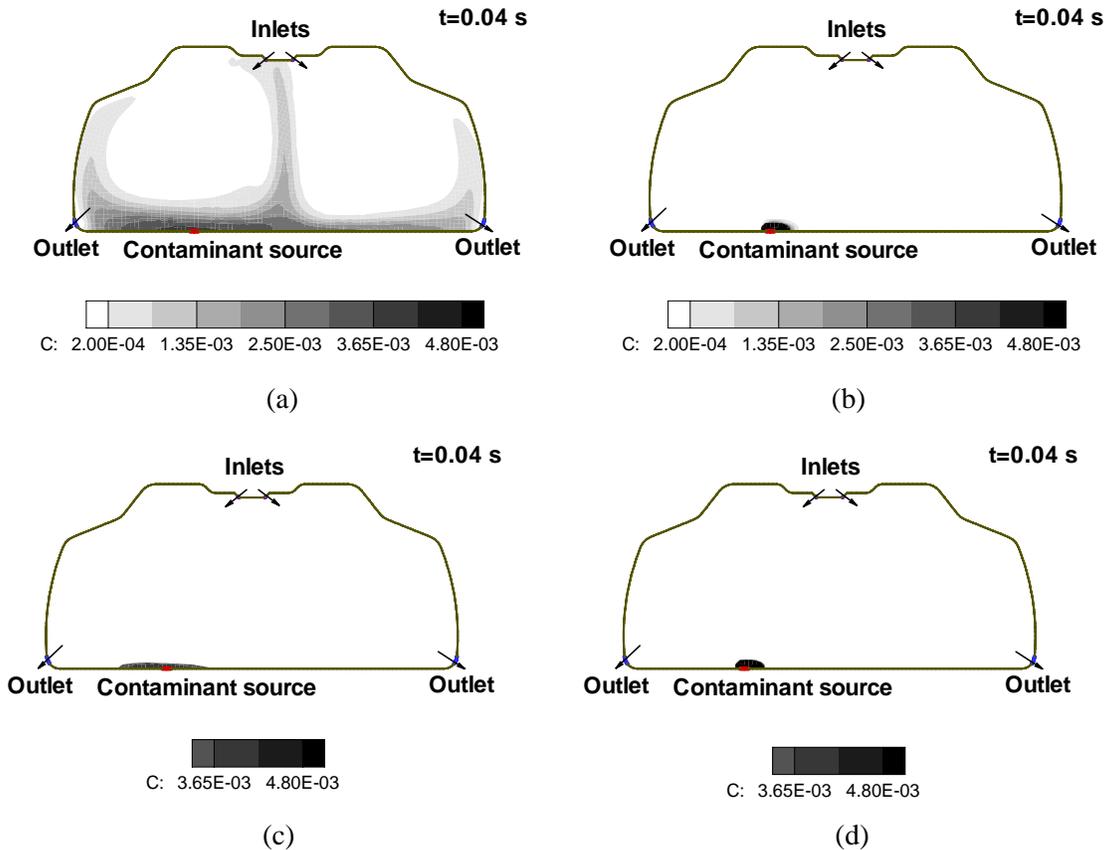
Fig.7 Comparison of the distributions of the contaminant concentration at $t = 0.04$ s (a) by the inverse CFD modeling, (b) by the direct CFD modeling, (c) peak concentration by the inverse CFD modeling, (d) peak concentration by the direct CFD modeling

13

In practice, it is often unknown when a contaminant is released. Inverse modeling could continue forever. Then it may not be possible to find the original source location and when it was introduced. This investigation has deliberately simulated the distribution of the contaminant concentration to $t = -2$ s with the inverse CFD modeling as shown in Figure 8. If there was a sensor at the left outlet in the cabin, it would measure some contaminant at $t = -2$ s because the outlet is at the downstream position of the peak concentration plume. If the sensor did not measure anything, Figure 8 is an impossible scenario. Then one would know that the source was introduced between t = -2 s ~ 0 s. Thus, the time when and location where the source were introduced can be identified. In other words, identification of the release location and time must be done together with boundary conditions, such as contaminant concentration from the outlets.
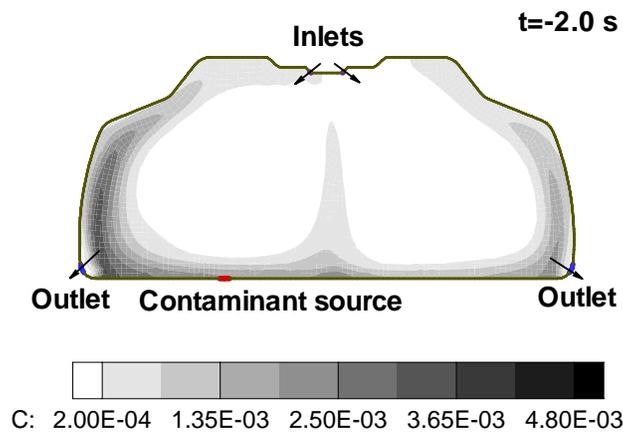
Fig. 8 The computed contaminant distribution at $t = -2$ s with the inverse CFD modeling

As shown in Figure 5, the airflow in the cabin was fully mixed at a very high air exchange rate. It took about 5 s to transfer the contaminant from the floor to the ceiling. A full circle of contaminant transport would take about 10 s. How could we know the contaminant was released 6 s ago or 16 s ago? According to the inverse modeling theory outlined in previous section, initial distributions of airflow and contaminant concentration are not the only condition for a successful inverse modeling. The inverse modeling needs boundary conditions, thermo-physical properties and geometric characteristics. For the aircraft cabin, the thermo-physical properties and geometric characteristics do not change over time in inverse modeling. Thus, boundary conditions are key factors in determining the release time.

This study also used the contaminant concentration distribution at $t = 16$ s as shown in Figure 9(a) as the initial conditions for the inverse CFD modeling. The contaminant distribution was calculated by direct CFD modeling (forward-time simulation). The distribution is very similar to that at $t = 6$ s shown as in Figure 6(b). Within 16 s, the contaminant has been transported in the cabin for one and a half circles. A part of the contaminant was exhausted from the two outlets. Figure 9(b) shows the contaminant concentration at the two outlets within 16 s. The concentration from the left outlet was higher than that from the right outlet because more contaminant was transported to the left side of the cabin. Since some contaminant had been exhausted out of the cabin, in inverse simulations the

extracted contaminant should be added back to the cabin as boundary conditions. Thus the contaminant concentration from the two outlets over time becomes crucial boundary conditions for the inverse modeling.

Figure 10(a) shows the distribution of contaminant concentration at $t = 0.04$ s, and Figure 10(b) shows the peak concentration at $t = 0.04$ s that were obtained by the inverse modeling with the initial distribution at t = 16 s and the boundary condition shown in Figure 9. Compared with Figure 7(a) and 7(c), the longer time of the inverse modeling, the more dispersive the results. This is not a surprise because the QR equation is dispersive. Nevertheless, the inverse modeling can still identify the contaminant source location.

(a)   (b)
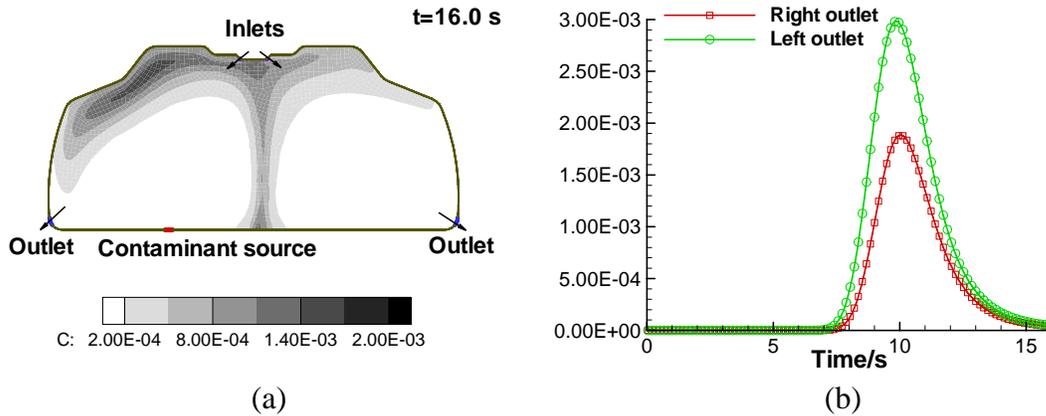
Fig. 9 Crucial conditions needed for the 16 s inverse modeling of the contaminant transport in the aircraft cabin (a) Initial distribution of the contaminant concentration in the cabin at $t = 16.0$ s, (b) contaminant concentration over time from the two outlets

(a)   (b)
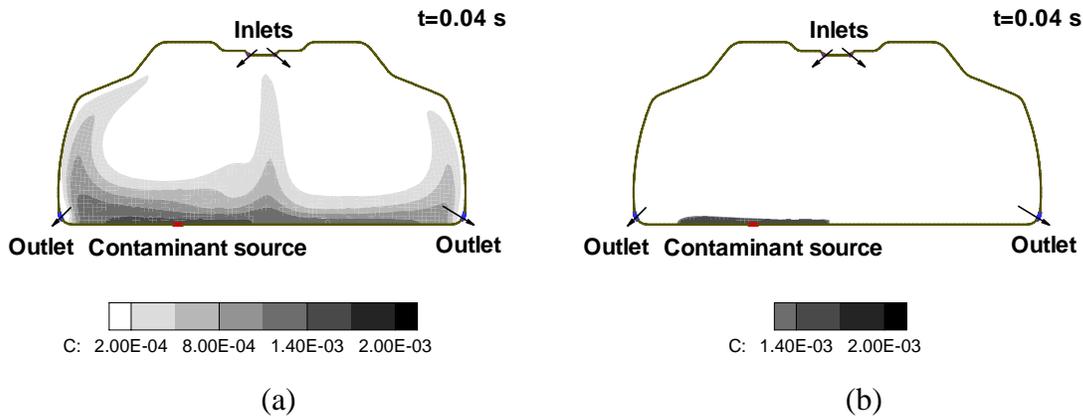
Fig. 10 The results from the 16 s inverse modeling for the aircraft cabin (a) The distribution of contaminant concentration at $t = 0.04$ s, (b) the peak concentration at $t = 0.04$ s

Application to a three-dimensional office

This investigation has also conducted inverse CFD modeling of contaminant transport in a three-dimensional office as shown in Figure 11 to further test the performance of the QR method and numerical scheme. The office was selected because we have done experimental measurements of airflow and contaminant transport in such a room simulated by an environmental chamber before (Yuan et al., 1999). The data has been used for validating our direct CFD results (Zhang and Chen, 2005). All the subjects in the office were simulated by rectangular boxes in both experimental measurements and CFD simulations. Conditioned air was supplied from a vertical diffuser located on the rear wall at the floor level, and the air was exhausted from the ceiling in the center of the room. The contaminant source was located at the head level of an occupant as shown in the figure. The contaminant was released from $t = 0$ - 0.04 s.
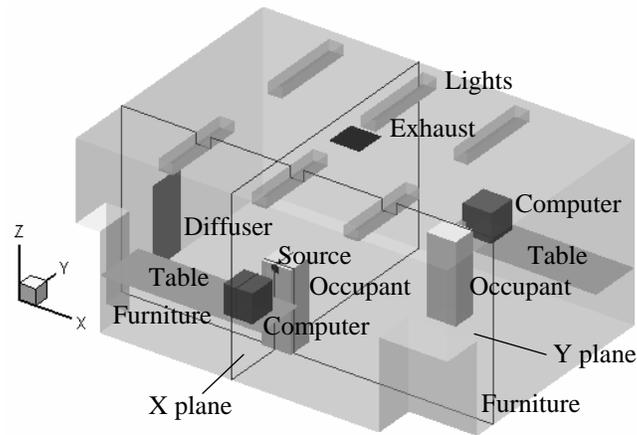
Fig. 11 The sketch of a three-dimensional office

The meshes for this office were created with *Submap* scheme. The size of the structured quad–CFD cells was about 0.1 m. Very similar to the previous case, this study used direct CFD modeling to obtain distributions of airflow and contaminant concentration at $t = 32$ s as initial data for inverse CFD modeling. The stabilization constant used was $\varepsilon=2.5\times10^{-5}$ m^4/s. Figure 12 shows the contaminant distributions in two planes across the occupant who released the contaminant. Unlike the aircraft cabin, the office was with a low air exchange rate and the ventilation scheme did not promote mixing. Thus, within 32 s the contaminant did not travel very far away from the occupant. Since no contaminant was transported to the exhaust, the contaminant concentration from the outlet remained zero in this period.
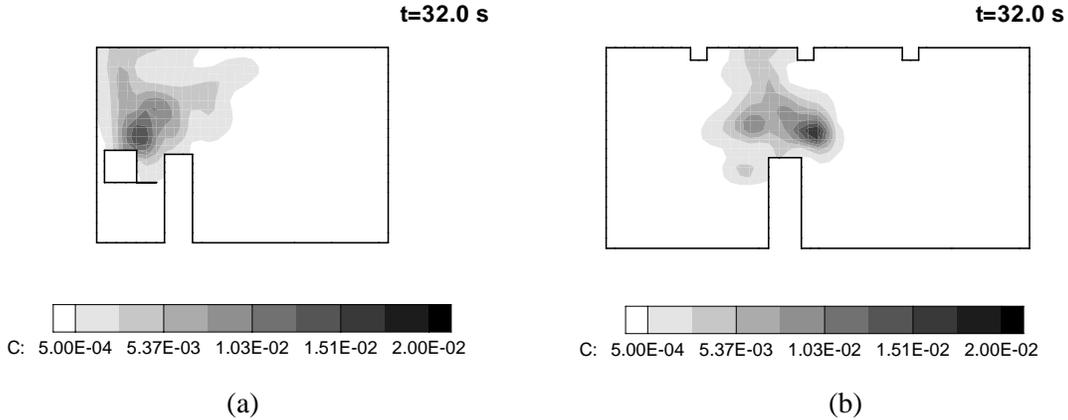
Fig. 12 The distributions of the contaminant concentration in the office after it was released for 32 s (a) on the X plane, (b) on the Y plane

Figure 13(a) and 13(b) illustrate the distributions of the contaminant concentration at $t = 0.04$ s on X and Y planes obtained by the inverse CFD modeling with the QR method. The results can indicate the contaminant source was located at the head level of the occupant, but the results are very dispersive. In this office, the air exchange rate was small. The diffusion played a much more important role than that in the aircraft cabin. Since the QR method solves Equation 3 that is not the same as the transport equation for contaminant concentration. Equation 3 does not have a correct term to represent diffusion. Thus, the error accumulated in the inverse modeling by solving Equation 3 became very significant in this case. The error was well reflected in the dispersive results shown in Figure 13.
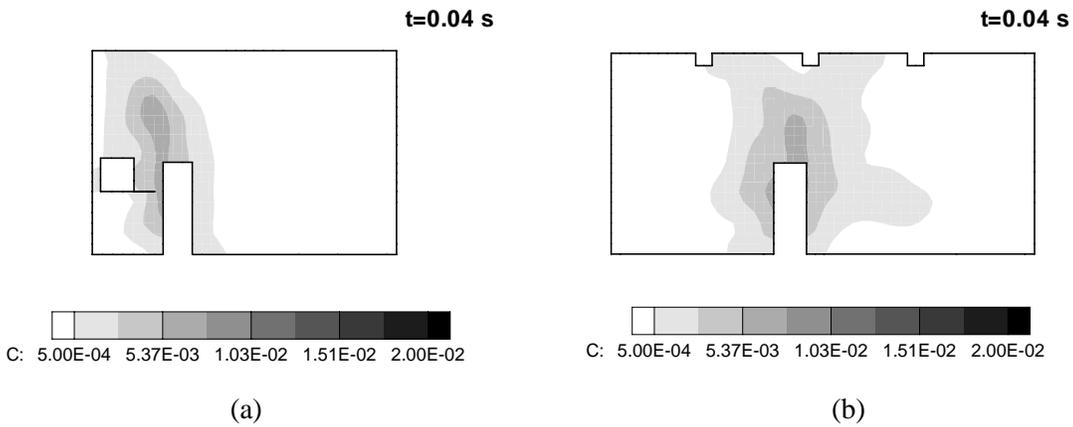
Fig. 13 The distributions of the contaminant concentration at $t = 0.04$ s in the office obtained with the inverse CFD modeling (a) on the X plane, (b) on the Y plane

Conclusions

This paper presented a new QR equation and numerical scheme to solve inversely contaminant transport in enclosed environments. By applying the new QR equation and numerical scheme to contaminant transport in a two-dimensional aircraft cabin and a three-dimensional office, the following conclusions could be drawn:

17

(1) The inverse CFD modeling with the new QR equation and numerical scheme can identify contaminant source locations. The contaminant strength becomes dispersive because the QR equation is not the transport equation for contaminants. The longer the simulation time, the more dispersive the results.

(2) In addition to initial distributions of airflow and contaminant concentrations, accurate boundary conditions over time at the outlets are crucial in determining contaminant source and strength for the case with contaminant exhausted out through the outlets.

(3) The new scheme can stabilize the inverse CFD modeling with unstructured meshes for the flow domain.

(4) The inverse CFD modeling with the QR equation works better for convection dominant flows. When the diffusion becomes important, the inversed CFD modeling can lead very dispersive contaminant concentration distributions.

Acknowledgements

Reference

Ala, N.K. and Domenico, P.A. (1992) Inverse analytical techniques applied to coincident contaminant distributions at Otis air force base, Massachusetts, *Ground Water.*, **30**, 212-218.

Alapati, S. and Kabala, Z.J. (2000) Recovering the release history of a groundwater contaminant using a non-linear least-squares method, *Hydrol. Process.*, **14**, 1003-1016.

Alifanov, O.M. (1994) *Inverse heat transfer problems*, New York, Springer-Verlag.

Arvelo, J., Brandt, A., Roger, R.P. and Saksena, A. (2002) An enhancement multizone model and its application to optimum placement of CBW sensors, *ASHRAE Trans.*, **108**, 818-825.

Atmadja, J. and Bagtzoglou, A.C. (2001) State of the art report on mathematical methods for groundwater pollution source identification, *Environ. Forens.*, **2**, 205-214.

Bagtzoglou, A.C., Dougherty, D.E. and Tompson, A.F.B. (1992) Application of particle methods to reliable identification of groundwater pollution sources, *Water Resour. Manage.*, **6**, 15-23.

Bagtzoglou, A.C. and Atmadja, J. (2003) Marching-jury backward beam equation and quasi-reversibility methods for hydrologic inversion: Application to contaminant plume spatial distribution recovery, *Water Resour. Res.*, **39**, SBH101-SBH1014.

Chen, Q. and Srebric, J. (2002) A procedure for verification, validation and reporting of indoor environment CFD analyses, HVAC&R Research., **8**, 201-216.

Clark, G.W. and Oppenheimer, S.F. (1994) Quasireversibility methods for non-well-posed problems, *Elec. J. Diff. Equations*, **8**, 1-9.

Enting, I.G. (2002) *Inverse problems in atmospheric constituent transport*, Cambridge, , Cambridge University Press .

Fluent Inc. (2005) *Fluent 6.2 UDF manual*, Fluent Inc.

Gorelick, S.M., Evans, B.E. and Remson, I. (1983) Identifying sources of groundwater pollution: an optimization approach, *Water Resour. Res.*, **19**, 779-790.

Kato S., Pochanart P. and Kajii Y. (2001) Measurements of ozone and nonmethane hydrocarbons at Chichi-jima island, a remote island in the western Pacific: long-range transport of polluted air from the Pacific rim region, *Atmos. Environ.*, **35**, 6021-6029.

Kato S., Pochanart P., Hirokawa J., Kajii Y., Akimoto H., Ozaki Y., Obi K., Katsuno T., Streets D.G. and Minko N.P. (2002) The influence of Siberian forest fires on carbon monoxide concentrations at Happo, Japan, *Atmos. Environ.*, **36**, 385-390.

Kato S., Kajii Y., Itokazu R., Hirokawa J., Koda S., Kinjo Y. (2004) Transport of atmospheric carbon monoxide, ozone, and hydrocarbons from Chinese coast to Okinawa island in the Western Pacific during winter, *Atmos. Environ.*, **38**, 2975-2981.

Kathirgamanathan, P., Mckibbin, R. and Mclachlan, R.I. (2002) Source term estimation of pollution from an instantaneous point source, *Res. Lett. Inf. Math. Sci.*, **3**, 59-67.

Lattes, R. and Lions, J.L. (1969) *The method of quasi-reversibility, applications to partial differential equations*, New York, Elsevier.

Mahar, P.S. and Datta, B. (2000) Identification of pollution sources in transient groundwater systems, *Water Resour. Manage.*, **14**, 209-227.

Mathur, S.R. and Murthy, J.Y. (1997) A pressure-based method for unstructured meshes, *Numer. Heat Tr. B*, **31**, 195-215.

Olsen, S.J., Chang, H.L., Cheung, T.Y., Tang, A.F., Fisk, T.L., Ooi, S.P., Kuo, H.W., Jiang, D.D., Chen, K.T., Lando, J., Hsu, K.H., Chen, T.J. and Dowell, S.F. (2003) Transmission of the severe acute respiratory syndrome on aircraft, *N. Engl. J. Med.*, **349**, 2416-2422.

Skaggs, T.H. and Kabala, Z.J. (1995) Recovering the history of a groundwater contaminant plume: Method of quasi-reversibility, *Water Resour. Res.*, **31**, 2669-2673.

Snodgrass, M.F. and Kitanidis, P.K. (1997) A geostatistical approach to contaminant source identification, *Water Resour. Res.*, **33**, 537-546.

Sohn, M.D., Reynolds, P., Singh, N. and Gadgil, A.J. (2002) Rapidly locating and characterizing pollutant releases in buildings, *J. Air & Waste Manage. Assoc.*, **52**, 1422-1432.

Sun, N.Z. (1994) *Inverse problems in groundwater modeling*, Boston, , Kluwer Academic.

Tikhonov, A.N. and Arsenin, V.Y. (1977) *Solutions of ill-posed problems*, Washington, DC, Halsted Press.

Venkatakrishnan, V. (1993) On the accuracy of limiters and convergence to steady state solutions, *AIAA*, **0880**, 1-10.

Wagner, B.J. (1992) Simultaneously parameter estimation and contaminant source characterization for coupled groundwater flow and contaminant transport modeling, *J. Hydrol.*, **135**, 275-303.

Wilson, J.L. and Liu, J. (1994) Backward tracking to find the source of pollution, *Water Manage. Risk Remed.*, **1**, 181-199.

Yuan, X., Chen, Q., Glicksman, L.R., Hu, Y. and Yang, X. (1999) Measurements and computations of room airflow with displacement ventilation, *ASHRAE Trans.*, **105**, 340-352.

Zhang, T. and Chen, Q. (2005) Comparison of different ventilation systems for commercial aircraft cabins, *Proc. Indoor Air 2005*, Beijing, China, **4**, 3205-3210.